THE NASA/AMES MARS GENERAL CIRCULATION MODEL: MODEL IMPROVEMENTS AND COMPARISON WITH OBSERVATIONS.

R.M. Haberle, *NASA/Ames Research Center (bhaberle@mail.arc.nasa.gov)*, **J.L Hollingsworth,** *NASA/Ames Research Center (jeffh@humbabe.arc.nasa.gov),* **A. Colaprete,** *NASA/Ames Research Center (tonyc@freeze.arc.nasa.gov)* **A.F.C. Bridger,** *San Jose State University (bridger@hellas.arc.nasa.gov),* **C.P. McKay,** *NASA/Ames Research Center (cmckay@mail.arc.nasa.gov),* **J.R. Murphy,** *New Mexico State University (murphy@nmsu.edu),* **J. Schaeffer**, *Raytheon Corporation (jschaef@mintz.arc.nasa.gov),* **and R. Freedman**, *NASA/Ames Research Center (freedman@darkstar.arc.nasa.gov).*

Introduction: For many years, the NASA/Ames Mars General Circulation Model (GCM) has been built around the UCLA B-grid dynamical core. An attached tracer transport scheme based on the aerosol microphysical model of Toon et al. (1988) provided a tool for studying dust storm transport and feedbacks (Murphy et al., 1995). While we still use a B-grid version of the model, the Ames group is now transitioning to the ARIES/GEOS Goddard C-grid dynamical core (Suarez and Takacs, 1995). The C-grid produces smoother fields when the model top is raised above 50 km, and has a built in transport scheme for an arbitrary number of tracers. All of our transport simulations are now carried out with the C-grid.

We have also been updating our physics package. Several years ago we replaced our bulk boundary layer scheme with a level 2 type diffusive scheme, and added a multi-level soil model (Haberle et al., 2000). More recently we replaced our radiation code with a more generalized two-stream code that accounts for aerosol multiple scattering and gaseous absorption. This code gives us much more flexibility in choosing aerosol optical properties and radiatively active gases. Thus, we have several versions of our GCM and these are listed in Table 1.

Table 1. Versions of the NASA/Ames Mars General Circulation Model.

Version	Dynamical Core	PBL / Soil Model	Radiation	Cloud Microphysics	Transport
1.0	B-grid	Bulk scheme / Single Layer	Dust/CO_2 - hardwired	H_2O clouds prescribed -fixed prop.	Aerosol model
1.5	B-grid	Level-2 scheme/ Multi-layer	Dust/CO_2 - hardwired	H_2O clouds prescribed -fixed prop.	None
1.7	C-grid	Level-2 scheme/ Multi-layer	Dust/CO_2 - hardwired	CARMA	C-grid advective scheme
2.0	C-grid	Level-2 scheme/ Multi-layer	Generalized 2-stream	Parameterized CARMA	C-grid advective scheme

GCM 1.0 was our original model but has been retired (though it is still available for comparison purposes). GCM 1.5 was used to interpret Pathfinder observations and was the first version of the model used to assess the effects of MOLA topography on the general circulation. GCM 1.7 is used to compare the differences between the B and C grids, and has also been coupled to a sophisticated cloud microphysics package (i.e., the Community Aerosol and Radiation Model for Atmospheres - CARMA, see Colaprete and Toon, 2000) to begin exploring water and CO_2 ice cloud formation. However, the version we are transitioning to is GCM 2.0, which is now undergoing final testing, and check out.

Model Improvements: The C-grid transport scheme advects tracers using the same numerical algorithm developed for potential temperature. At present, we use this scheme to transport water vapor, and an arbitrary number of dust and cloud particles. Dust can be lifted into the atmosphere through a prescribed source, or a model-predicted parameterization. Once into the lowest layer (nominally 10 m thick) dust is vertically mixed by a stability dependent diffusive scheme followed by a convective adjustment. Water vapor is treated similarly, though we do not yet have a good evaporation parameterization for surface ice. Dust is removed by gravitational settling; water vapor by precipitation. The latter can range in sophistication from simple successive saturation removal, to a full up CARMA cloud microphysical approach.

The model-predicted dust lifting schemes are based on the work of Murphy (1999) (with details given in Haberle et al., 2002) and Newman et al.

(2002). Murphy's lifting scheme is parameterized in terms of surface stress, whereas the Newman et al. scheme is based on a saltation flux calculated from the friction velocity. Both schemes are threshold schemes.

GCM versions < 2.0 use a radiation code that is hard-wired to specific dust and water ice optical properties, with CO_2 being the only radiatively active gas. Furthermore, the range of surface pressures this code can accommodate is limited to < 100 hPa. Our new radiation code is based on a generalized two-stream solution to the radiative transfer equation with gaseous opacities calculated using correlated-k's. The two-stream solutions can accommodate Eddington, Quadrature, Hemispheric Mean, and Delta function approximations. We are presently using the Quadrature approximation for solar radiation and the energy conserving Hemispheric Mean approximation in the thermal infrared.

At present we run with 34 spectral intervals from 0.3 to 250 microns. The correlated-k's for these intervals are generated from a line-by-line code using the HITEMP data base from HITRAN for CO_2, and a version of the Schwenke data base (to include lines too weak to appear in HITRAN) for H_2O. In both cases line widths are adjusted to represent CO_2 broadening. A Voigt profile is used at low pressures, and a Lorentz profile at high pressures. The line widths are extended at high pressures so as to include all significant absorption. The abundance of the deuterated species for H_2O was adjusted for Mars conditions. The line-by-line calculations were then windowed, and sorted to produce the k coefficients. We use a gauss scheme of 8 & 8 points in each spectral interval with the dividing point at .95 to extract the actual coefficients from the sorted probability distribution. The k coefficients have been computed for a range of pressures, temperatures, and relative humidities that allows us to simulate past as well as present Martian climates. A example of how this new code compares with Dave Crisp's DART code for a pure CO_2 atmosphere is shown in Fig. 1.

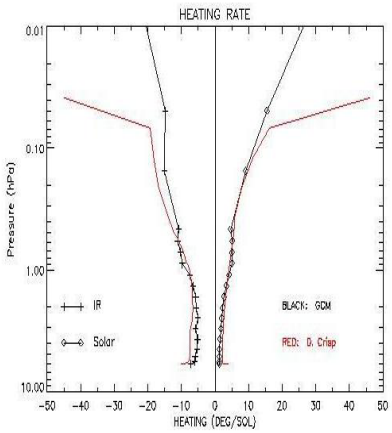

Figure 1 : Solar and IR heating rates computed from the new radiation code (black) and Crisp's DART code**.**

For aerosols, we calculate the wavelength dependent scattering properties (ω_o, g, and Q_{ext}) off line using Mie theory. The dust scattering properties we are presently using are taken from the Ockert-Bell et al. (1997) work in the visible and Forget (1998) in the infrared. The visible (.67 microns) to infrared opacities are scaled to produce a value of 2 at 9 microns.

During the past several years we have coupled the CARMA cloud microphysics package into the C-grid (GCM version 1.7) and have begun exploring the behavior of H_2O and CO_2 ice clouds in the present climate system (e.g., Colaprete and Haberle, 2001). The microphysics model accounts for the particle-size dependent processes of nucleation, condensation, sedimentation, and evaporation. The expressions used for these processes and the rationale for them are given in Colaprete (2000) and references therein. The model keeps track of three particle types in an arbitrary number of size bins: dust, ice, and ice-coated dust. The ice can be water ice or CO_2 ice. The code is general enough to handle both.

Comparison with Observations: We have been comparing GCM 1.5, 1.7, and 2.0 with Viking and MGS observations. With GCM 1.5 we were able to pin down the annual global mean surface pressure on Mars. We tuned the polar cap properties until the model-predicted surface pressures gave a good fit to the Viking Lander 1 and 2 data (Fig. 2). The resulting global mean annual surface pressure was 6.1 hPa, coincidentally (?) indistinguishable from the triple point pressure of water.

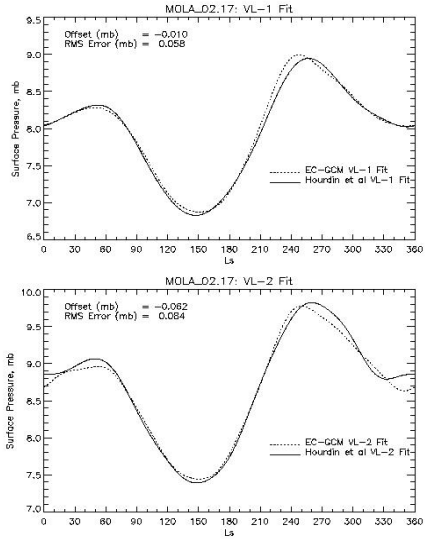

Figure 2 : GCM fit to daily averaged Viking Lander surface pressures

These simulations have also been compared to TES temperature data, where we find reasonable agreement with zonal mean values, but significant differences with the inferred amplitudes of the winter stationary waves. TES data show winter wave 1 amplitudes of ~8K in both hemispheres (Banfield et al.,

2002), whereas our fixed dust and globally uniform GCM simulations produce ~20K in the south and ~ 4K in the north. We can beat down the wave 1 amplitudes in the south by either lowering the global opacity to ~ 0.1, or by running with a relatively clear polar atmosphere. The latter is more realistic. In the north however, the 4K amplitudes are robust to changes in the dust distribution. The northern amplitudes increase somewhat when the center of the time averaging window is moved a little earlier or later in the season. But the amplitudes never reach the 8K seen in the TES data. Figure 3 shows our GCM results when we run using the TES observed opacities.

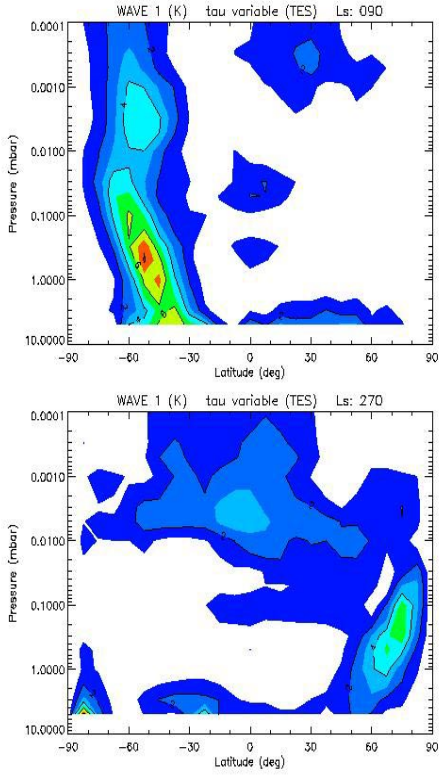

Figure 3 : Stationary wave 1 temperature amplitudes for southern winter (top) and northern winter (bottom).

To compare the model results with observed dust storm activity we introduce the concept of a deflation potential, which we define as the depth of dust that could be removed from the surface during a specified period of time. The deflation potential from one of our fixed dust (tau=0.3) experiments based on the Murphy (1999) lifting parameterization for the period between L_s=109°-274° is shown in Fig. 4. Also shown are Cantor et al's (2001) observations of local dust storms by the MOC wide angle camera during the same period. Both model and observations show that dust lifting occurs mostly poleward of 30° in either hemisphere. There is also a modest correlation between the density of dust storms and the magnitude of the deflation potential. The distribution of observed dust storms is more or less longitudinally uniform in both hemispheres, which is consistent with model predictions in the Northern Hemisphere, but less so in the Southern Hemisphere. Interestingly, very little lifting is predicted in the tropics (between ±30°) where only a few dust storms were observed. Overall, the model compares remarkably well with observations considering the assumptions of uniform surface roughness, threshold stress, and atmospheric dust loading.

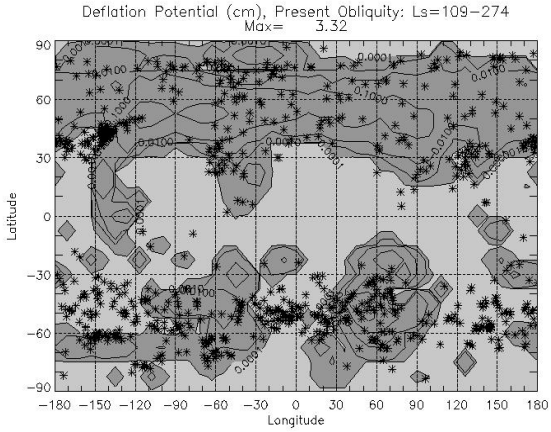

Figure 4 : Deflation potential (contours) and dust storms (stars).

An example of our fully coupled GCM and cloud microphysical model is shown in Fig. 5. In this simulation we employ the full capability of CARMA and carry 6 dust bins, 6 cloud bins (water and CO_2), and 1 water vapor bin. The figure depicts the zonally-averaged mass-weighted mean water ice cloud particle sizes at Ls=103°. The tropical aphelion cloud belt is readily simulated. Most of the water for these clouds comes from the subliming

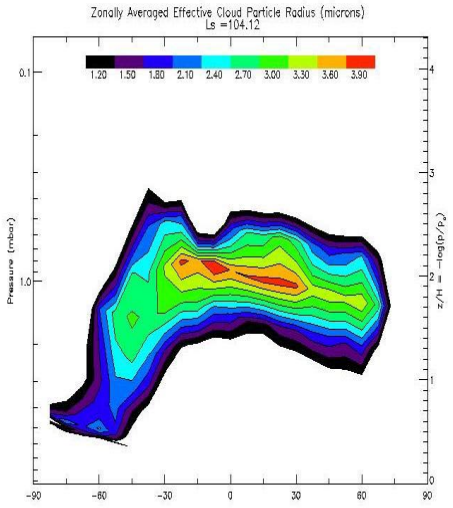

Figure 5 : Zonally-averaged ice cloud particle sizes from a simulation using CARMA.

north polar residual ice cap. The water is transported off the cap at low levels and is then swept up in the

ascending branch of the Hadley circulation where it is quickly transported into the southern hemisphere. Some of this water precipitates out as it moves across the equator thereby moistening the lower atmosphere. Once into the southern hemisphere, the remaining water is moved back toward the surface in the descending branch of the Hadley circulation where some of it condenses out onto the seasonal CO_2 ice cap which extends to about 60°S in this simulation.

One aspect of the observations, which our model does not compare well with, is the thermal tides. The amplitudes of our diurnal and semidiurnal surface pressure tides are significantly lower than observed at either Viking lander site, or the Pathfinder site. Though this is not necessarily a serious flaw, the fact that other GCMs do find good agreement has motivated us to better understand the reason for our weaker tides. Given the sensitivity of the tides to dust heating, this is the obvious thing to explore first. So we have begun simulations with GCM 2.0 to determine the tidal response to different assumptions about the dust radiative properties. We hope to report these results at the workshop.

References:

Banfield, D., B.J. Conrath, J. Pearl, M.D. Smith, P.R. Christensen, and R. John Wilson, 2002. Forced Waves in the Martian atmosphere from MGS TES Nadir data. *Icarus*, In Press.

Cantor, B.A, P.B. James, M. Caplinger, and M.J. Wolff 2001. Martian dust storms: 1999 Mars Orbiter Camera observations. J. *Geophys. Res*. In press.

Colaprete, A. 2000*: Clouds on Mars*. Ph.D. Thesis, University of Colorado. 149 p.

Colaprete, A., and R. Haberle, 2001: Initial results from the NASA/Ames GCM Carbon Dioxide cloud model. Abstract, XXVI European Geophysical Society meeting, Nice, France.

Haberle, R.M., J.R. Murphy, and J. Schaeffer 2002. Orbital change experiments with a Mars General Circulation Model. *Icarus*. In press.

Murphy, J.R. 1999. The Martian atmospheric dust cycle: Insights from numerical model simulations. Fifth International Conference on Mars. Abstract 6087. Lunar and Planetary Institute, Houston TX.

Newman, C.E., S.R. Lewis, and P.L. Read 2002. Modeling the Martian dust cycle. : Representations of dust transport processes, J. Geophys. Res., In press.

Ockert-Bell, M.E., J.F. Bell III, J.B. Pollack, C.P. McKay, and F. Forget, 1997: Absorption and scattering properties of the Martian dust in the solar wavelengths, *J. Geophys. Res*., **102**, 9039-9050.

Toon, O.B, R.P. Turco, D. Westphal, R. Malone, and M.S. Liu, 1988. A multidimensional model for aerosols: Description of computational analogs, *J. Atmos. Sci.,* **45**, 2123-2143.

Toon, O.B, C.P. McKay, and T.P. Ackerman, and K Santhanam,1989: Rapid calculation of radiative heating rates and photodissociation rates in inhomogeneous multiple scattering atmospheres, *J. Geophys. Res*., **94**, 16287-16301.